

⁵L. Andrews and G. C. Pimentel, *J. Chem. Phys.* **47**, 2905 (1967).

⁶S. L. Kupferman and F. M. Pipkin, *Phys. Rev.* **166**, 207 (1968).

⁷A. A. Belyaeva, Y. B. Predtechenskii, and L. D. Shcherba, *Izv. Akad. Nauk SSSR, Ser. Fiz.* **33**, 895 (1969) [*Bull. Acad. Sci. USSR, Phys. Ser.* **33**, 825

(1969)].

⁸H. Coufal, M. Burger, U. Nagel, E. Lüscher, K. Boning, and G. Vogl, *Phys. Lett.* **48**, 1433 (1974).

⁹J. F. Dawson and L. C. Balling, to be published.

¹⁰W. E. Baylis, *J. Chem. Phys.* **51**, 2665 (1969).

¹¹J. Pascale and J. Vandeplanque, *J. Chem. Phys.* **60**, 2278 (1974).

Experimental Observation of Current Generation by Unidirectional Electron Plasma Waves

K. L. Wong

Plasma Physics Laboratory, Princeton University, Princeton, New Jersey 08540

(Received 10 July 1978; revised manuscript received 5 June 1979)

A slow-wave structure was used to launch electron plasma waves traveling preferentially in one direction. The current generated by the waves was observed. The magnitude of the current can be estimated from momentum conservation in the wave-particle interaction process.

Plasma currents driven by traveling waves were first observed by Thonemann, Cowhig, and Davenport¹ in 1952, and the experiment was later repeated; see Bozunov *et al.*² and Demirkhanov *et al.*,³ also Fukuda.⁴ In principle, any wave with a net momentum can generate a current via any damping mechanism caused by the charged particles in the plasma. Ion cyclotron waves have been used to produce a current in the Princeton Model-C stellarator,⁵ and current generation by whistler waves⁶ has been reported recently. The application of rf-driven current to steady-state tokamak reactors has been considered by a number of authors.⁷⁻¹⁰ If the current is carried by the main-body electrons, the rf power becomes too large to be practical.^{7,10} Recently it was proposed to generate a current carried by the electrons in the tail of the distribution function¹⁰ via Landau damping of lower-hybrid waves.^{11,12} This idea relies upon the momentum transferred from the waves to the tail electrons and therefore requires unidirectional waves which can be generated by 90° phased metal plates or wave-guide arrays.¹³ In this paper I report the first experimental observation of current generation by the unidirectional electron plasma waves via wave-particle interaction. Electron plasma waves are called lower-hybrid waves when the wave frequency is near the lower hybrid frequency. These waves are attractive to magnetic fusion research due to the desirable features of the launching structure (phased wave-guide arrays) and the readily available technology to produce the necessary rf power corresponding to the tokamak reactor parameters.

Consider the electron plasma wave which obeys the following dispersion relation:

$$\omega = \frac{k_z}{k} \frac{\omega_{pe}}{(1 + \omega_{pe}^2/\omega_{ce}^2)^{1/2}}, \quad (1)$$

where k_z is the wave number along the magnetic field; k is the total wave number; ω , ω_{pe} , and ω_{ce} are the wave frequency, the electron plasma frequency, and the electron cyclotron frequency, respectively. Let E_0 be the electric field amplitude of the wave and let ϵ be the plasma dielectric function. The parallel component of the wave momentum density is

$$P_z = \frac{E_0^2}{16\pi} \frac{\partial}{\partial \omega} (\omega \epsilon) k_z = \frac{1}{8\pi} E_0^2 \frac{k_z}{\omega} \left(1 + \frac{\omega_{pe}^2}{\omega_{ce}^2} \right). \quad (2)$$

If the wave momentum is absorbed by the electrons, it will generate a current density

$$J_z = \frac{e}{m} \frac{E_0^2}{8\pi} \frac{k_z}{\omega} \left(1 + \frac{\omega_{pe}^2}{\omega_{ce}^2} \right), \quad (3)$$

where e/m is the electron-charge-to-mass ratio. In a toroidal plasma, the resonant electrons moving parallel to the magnetic field are confined. The wave-generated current will increase as long as there is a nonzero slope in the electron velocity distribution function for Landau damping until electron-ion collision transfers the electron momentum into the ions. In linear machines, the resonant electrons leave the plasma through the end of the machine before electron-ion collisions occur. Consider a pulsed wave packet of power P_w and pulse length τ . If the wave is completely damped by electrons, the total charge that leaves

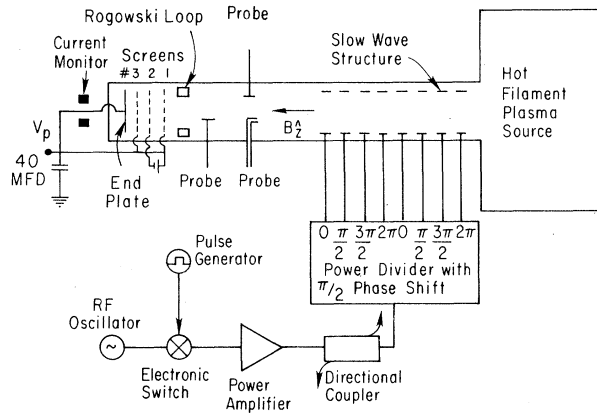


FIG. 1. Schematic of experimental setup. The plasma column is about 260 cm long. The slow-wave structure is about 145 cm from the end plate.

the plasma because of end loss is

$$Q = I\tau = (e/m)P_w\tau(k_z/\omega)^2, \quad (4)$$

where I is the current generated by the waves. The loss of electrons will create an ambipolar potential in the plasma which tends to transfer the electron momentum into the ions. Fortunately, the hot-filament plasma source can provide electrons to replace those forced out by the waves. If the distance L between the antenna and the end of the machine is not much shorter than the collisional mean free path L_c for the resonant electrons, then, the wave-generated current measured at the end of the machine can be estimated by

$$I = (e/m)P_w(k_z/\omega)^2 \exp[-(L - \frac{1}{2}L_d)/L_c], \quad (5)$$

where $L_d < L \sim L_c$ is the damping length of the wave.

The experiment was performed in the Princeton $L-3$ device with the following parameters: Magnetic field $B \sim 1.3$ kG, plasma density $n \sim (1-4) \times 10^{10} \text{ cm}^{-3}$, electron temperature $T_e \sim 3$ eV, and ion temperature $T_i < 0.1$ eV. The neutral pressure was about 2×10^{-4} Torr, and the argon plasma was produced by a hot multifilament source. The slow waves were launched by a 14-cm-long slow-wave structure¹¹ consisting of eight rings driven by an rf oscillator. The rf power divider imposes a 90° phase difference between adjacent rings so that the waves propagate preferentially in one direction. Figure 1 shows a schematic of the experimental setup. To identify the waves excited by the antenna, a boxcar integrator was used to measure the wave electric field at a sequence of times by a sampling technique.¹¹ The data shown

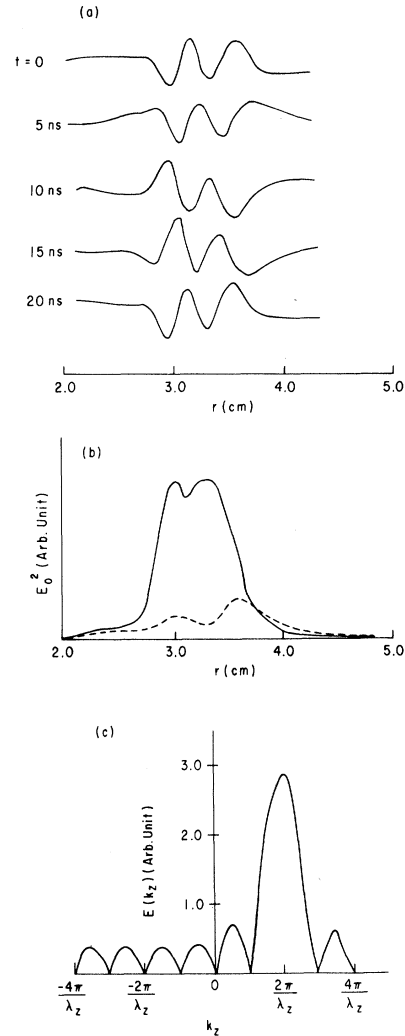


FIG. 2. (a) Wave electric field at a sequence of times measured by the sampling technique with density $n \approx 10^{10} \text{ cm}^{-3}$, parallel wavelength $\lambda_z \approx 7$ cm, wave frequency $f \approx 50$ MHz, magnetic field $B \approx 1.3$ kG. (b) Wave amplitude profile (E_0^2 vs r) on the two sides of the antenna, the solid line is for the wave at the preferred direction. (c) Calculated spectrum for the slow-wave structure.

in Fig. 2(a) clearly indicate that the waves obey the dispersion relation given in Eq. (1). It is apparent that the phase velocity of the waves is propagating radially outward while the wave energy propagates inward. This is because it is a backward wave in the radial direction which is a characteristic of electron plasma waves. Figure 2(b) shows the amplitude profile of the waves on the two sides of the antenna. It is apparent that about 85% of the power ($P_w \propto E_0^2$) propagates in one direction which agrees with the calculated spectrum shown in Fig. 2(c). The net power P_{rf}

transmitted by the antenna can be precisely measured by a calibrated dual directional coupler, but the fraction that goes into the electron plasma waves cannot be accurately determined. A double-tip probe was used to measure the wave electric field in the plasma. The sensitivity of the probe was calibrated in an electric field between two parallel metal plates driven by an oscillator at the same frequency as the electron plasma waves. Based on probe measurements, we estimate that $p_w \sim (0.3-0.9)P_{rf}$. The wave is damped as it propagates along the resonance cone [see Fig. 3(a)]. A ferrite-core current monitor¹⁴ (20-ns rise time, 1.0-V/A sensitivity, 0.06%/μsec droop) was used to measure the wave-generated current collected by the end plate which was connected to ground through a 40-MF capacitor held at the plasma potential V_p . The capacitance is large enough so that the charge collected by the end plate does not change the plate potential significantly. Three metal mesh grid (No. 1, No. 2, and No. 3 shown in Fig. 1) were put in front of the end plate with transparencies of 50%, 50%, and 90%, respectively. For various combination of grids, the current collected by the end plate is reduced by the amount that corresponds to the grid transparency. By biasing the grids as an electrostatic energy analyzer, the current carrying electrons were found to be in the same energy range of the resonant electrons (10–80 eV) of the launched electron plasma waves. At high rf power levels (≥ 100 W), the plasma potential may change by a few volts and eject low-energy (a few eV) electrons towards the end plate. In this experiment, the rf power was kept below 20 W to minimize this effect. In addition, the grids were biased to reject electrons below 10 eV so that the collected current was carried by the resonant electrons. A Rogowski loop calibrated with a known 400-ns current pulse was used to double check the current monitor measurement. They usually agree within 20%. Since the Rogowski loop has slow response time ($\sim 0.4 \mu\text{s}$), all the data presented here are based on the current monitor measurements. Figure 3 shows the wave damping along the resonance cone and the current generated by a short (400 ns) rf pulse. The arrival time of the current peak approximately corresponds to the time of flight of the resonant electrons ($V_z \sim 3.5 \times 10^8 \text{ cm/s} \sim 3V_{Te}$). This has been verified for various antenna locations and it is consistent with the results from previous investigation¹¹ of Landau damping of electron plasma waves in this device (L-3). At such a low

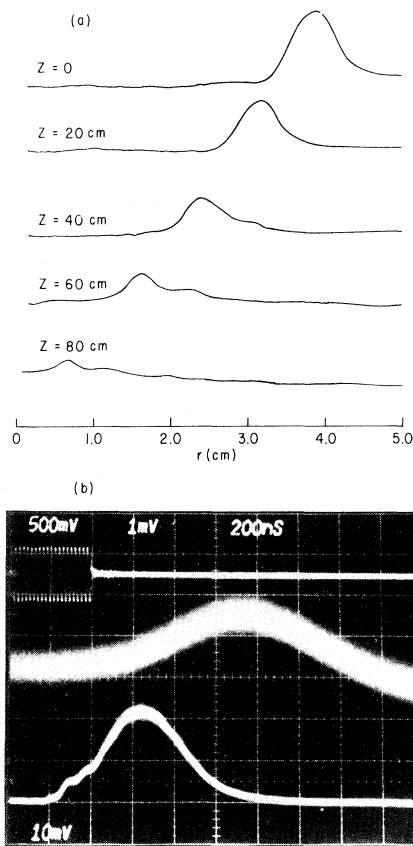


FIG. 3. (a) Wave amplitude profiles (E_0^2 vs r) at various axial locations with $\lambda_z \approx 7 \text{ cm}$, $f \approx 50 \text{ MHz}$, $p_{rf} \approx 20 \text{ W}$, and $n \approx 2 \times 10^{10} \text{ cm}^{-3}$. (b) The top trace shows the 400-ns rf pulse, the middle trace shows the Rogowski loop signal, and the bottom trace shows the current monitor signal.

velocity, the electron-neutral collisional mean free path becomes comparable to the distance between the antenna and the end plate so that collisional attenuation should be taken into account. The total charge Q collected by the end plate can be obtained by integrating the current signal. The wave-generated current ($I = Q/\tau$) was found to be proportional to the power level of the rf pulse as shown in Fig. 4. If one assumes $P_w = 0.35P_{rf}$, the current predicted by Eq. (5) agrees very well with the experimental data. As expected, the current drops rapidly with increasing neutral pressure and it is independent of the plasma density as long as the waves are totally damped before they reach the end plate.

In conclusion, we have observed experimentally that currents can be generated via damping of unidirectional slow waves and the magnitude of the current can be estimated from momentum

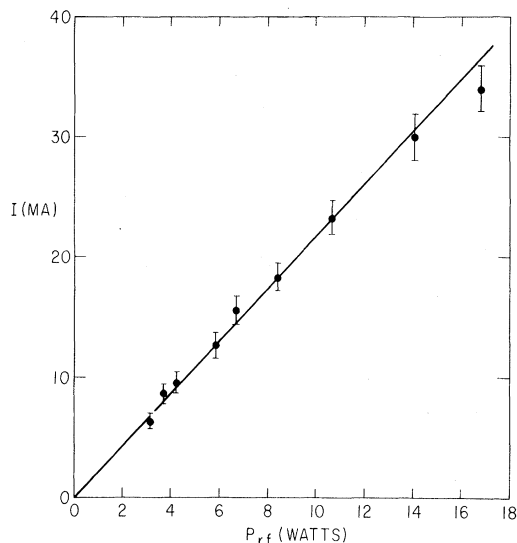


FIG. 4. Total current generated by the waves as a function of rf power with $\lambda = 7$ cm, $f = 50$ MHz, $\tau = 400$ ns, and $n \approx 2 \times 10^{10}$ cm $^{-3}$. The solid line represents the current calculated from Eq. (5) with the assumption that $P_w = 0.35P_{rf}$.

conservation in the wave-particle interaction. In order to generate a steady-state current for toroidal plasma confinement, one has to rely upon electron collisions to maintain a nonzero slope in the electron distribution function which is necessary for Landau damping. The feasibility of employing this mechanism to operate a steady-state tokamak remains to be proved in toroidal plasma experiments.

The author would like to thank Dr. M. Ono for his calculation of the k spectrum of the slow-wave structure as well as many helpful ideas. Discussions with Dr. M. Porkolab and Dr. N. Fisch, and technical assistance by Mr. J. R.

Wilson and Mr. J. Taylor, are gratefully appreciated.

This work was supported by the U. S. Department of Energy Contract No. EY-76-C-02-3073.

¹P. G. Thonemann, W. T. Cowhig, and P. A. Davenport, *Nature* **169**, 34 (1952).

²N. A. Bozunov, N. Ya. Kuzimina, I. Kh. Nevyazhskii, S. M. Osovets, Yu. F. Petrov, B. I. Polyakov, I. A. Popov, K. V. Khodataev, and V. P. Shimchuk, *Dokl. Akad. Nauk SSSR* **152**, 581 (1963) [*Sov. Phys. Doklady* **8**, 914 (1964)].

³R. A. Demirkhanov, I. Ya. Kadysh, I. S. Fursa, and Yu. S. Khodyrev, *Zh. Tekh. Fiz.* **35**, 212 (1965) [*Sov. Phys. Tech. Phys.* **10**, 174 (1965)].

⁴M. Fukuda, K. Matsuura, K. Hirano, A. Mohri, and M. Fukao, *J. Phys. Soc. Jpn.* **41**, 1376 (1976).

⁵S. Yoshikawa and H. Yamato, *Phys. Fluids* **9**, 814 (1966).

⁶R. Klima, V. Kopecky, J. Musil, F. Zacek, P. Heymann, and A. M. Ternopol, *Phys. Lett.* **65A**, 23 (1978).

⁷T. Ohkawa, *Nucl. Fusion* **10**, 185 (1970).

⁸D. J. H. Wort, *Plasma Phys.* **13**, 258 (1971).

⁹R. Klima, *Plasma Phys.* **15**, 1031 (1973).

¹⁰A. Bers and N. Fisch, in *Proceedings of the Third Topical Conference on Radio Frequency Plasma Heating*, Pasadena, January 1978, (unpublished), papers E-5 and E-6; also N. Fisch, Research Laboratory of Electronics, Massachusetts Institute of Technology, Report No. PRR 78/9 (unpublished).

¹¹P. Bellan and M. Porkolab, *Phys. Fluids* **19**, 995 (1976).

¹²F. J. Paoloni, R. W. Motley, W. M. Hooke, and S. Bernabei, *Phys. Rev. Lett.* **39**, 1081 (1977).

¹³S. Bernabei, M. Heald, W. Hooke, R. Motley, F. Paoloni, M. Brambilla, and W. Getty, *Nucl. Fusion* **17**, 929 (1977).

¹⁴Current monitor Model 2100 manufactured by Pearson Electronics, Inc., Palo Alto, California.

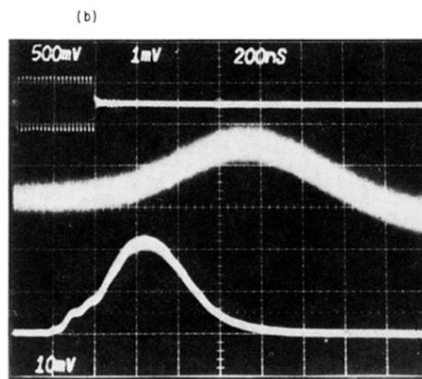
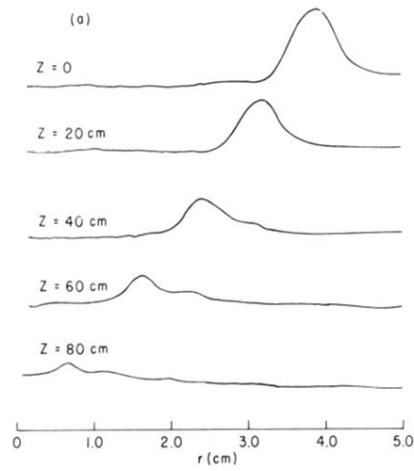


FIG. 3. (a) Wave amplitude profiles (E_0^2 vs r) at various axial locations with $\lambda_z \approx 7$ cm, $f \approx 50$ MHz, $p_{rf} \approx 20$ W, and $n \approx 2 \times 10^{10}$ cm $^{-3}$. (b) The top trace shows the 400-ns rf pulse, the middle trace shows the Rogowski loop signal, and the bottom trace shows the current monitor signal.